

Discharge Chamber Performance of the NEXIS Ion Thruster

Dan M. Goebel, James Polk, and Anita Sengupta

Jet Propulsion Laboratory, California Institute of Technology, Pasadena, CA 91109

The Nuclear-Electric Xenon Ion System (NEXIS) thruster was designed to produce $\geq 70\%$ efficiency at ISPs in excess of 6500 sec and total power levels in excess of 15 kW. In order to achieve this performance, the thruster requires a large area plasma generator capable of high propellant utilization efficiency and low discharge loss while producing a very flat, uniform beam profile. Fortunately, larger thrusters can be made more uniform and efficient due to the higher volume to surface ratio, provided that the magnetic cusp confinement is designed properly and the thruster length to diameter ratio is adequate. This paper describes the discharge chamber performance of the NEXIS "Laboratory Model" (LM) thruster. The LM discharge chamber is 65 cm in diameter at the grid plane and uses 6 ring-cusps to provide magnetic confinement of the plasma. The thruster was tested with flat carbon-carbon composite grids with the hole pattern masked to 57 cm in diameter and a conventional Type-B "1/2" diameter hollow cathode. During the preliminary "discharge only" tests, the LM thruster demonstrated profile factors of 0.84 and a discharge loss of about 160 eV/ion at 25 V discharge voltage and over 90% propellant utilization efficiency in simulated beam extraction experiments at 3.9 A of beam current. Analysis of the data from these tests used the "discharge-only" model developed by Brophy¹. Subsequent beam extraction experiments validated the key variables used in the model to predict the performance from the "discharge-only" data, and demonstrated 3.9 A of beam current at over 90% propellant utilization efficiency with a flatness parameter of better than 0.8 and a discharge loss of about 185 eV/ion. The slightly higher discharge loss measured during beam extractions was found to be due to a lower screen transparency in the as-manufactured LM grid set. Plasma measurements with a scanning probe internal to the thruster near the screen grid showed plasma densities over $1 \times 10^{11} \text{ cm}^{-3}$ and electron temperatures of 3.5 to 5.5 eV depending on the operation parameters. The performance of the NEXIS discharge chamber contributed to the over 78% thruster efficiency measured during beam extraction at 7500 sec ISP and 25 kW of power, and over 81% thruster efficiency measured at 8500 sec ISP.

Nomenclature

A	= probe area
e	= electron charge
f_a	= fraction of ions striking the accelerator grid that leave the discharge chamber as neutrals
I	= probe current
k	= Boltzman's constant
n	= plasma density
m	= electron mass
M	= ion mass
\dot{m}	= discharge flow rate in equivalent amperes
ϕ_i	= grid transparency with high voltage applied
ξ	= dimensionless correction for thick sheath regime
λ_D	= deBye length in the plasma
η_m	= mass utilization efficiency
η_D	= discharge loss

I_{sp}	=	specific impulse
J_D	=	discharge current
J_K	=	keeper current
J_s	=	ion current to the screen grid
J_a	=	ion current to the accelerator grid
J_g	=	total grid plane ion current
J_b	=	ion current leaking through the grids
T_e	=	electron temperature
V_D	=	discharge voltage
V_K	=	keeper voltage
V_p	=	probe potential
V	=	probe potential relative to plasma potential

I. Introduction

The NEXIS laboratory model thruster^{2,3} design is based on the NSTAR⁴ and Xenon Ion Propulsion System (XIPS)⁵ ring-cusp thruster concepts⁶⁻⁸ that utilize a hollow cathode discharge to produce the plasma, magnetic-multipole ring-cusps to confine the plasma, and multi-aperture grids to accelerate the xenon ions to produce thrust at high specific impulse (I_{sp}). NEXIS also utilizes carbon-carbon composite grids⁹ and a graphite keeper electrode to provide long life with a high throughput. The original "single-design-point" goal for the thruster was to produce an efficiency of 78% at an ISP of 7500 sec and total power of about 22 kW. It was also desired for the thruster to operate at I_{sp} s in the range of 6500 sec to 8500 sec with high efficiency and total power levels of 15 to 25 kW. In order to achieve such a high efficiency and this large range of I_{sp} , the discharge chamber was required to provide high propellant utilization efficiency and low discharge loss while producing a very flat, uniform beam profile. This paper describes the performance of the NEXIS "Laboratory Model" (LM) thruster discharge chamber.

The Laboratory Model (LM) thruster was tested first in a "discharge-only" mode to validate the discharge chamber and cathode design, and provide preliminary thruster performance data for the JIMO system design teams. Discharge-only mode tests consist of full operation of the main discharge in the plasma chamber to produce the xenon plasma in the thruster, but the xenon ions arriving at the grid structure are collected and not accelerated to form a beam. This mode of operation requires that significantly less gas be injected into the thruster than normal because a large fraction of the ions that are collected by the grids are returned into the thruster as neutrals. The electrical and gas flow parameters recorded during this test are then used to calculate the thruster performance (beam current, mass utilization efficiency, discharge loss, etc.) that will be obtained during high voltage beam extraction using a model developed by Brophy¹. The NEXIS thruster performance from these tests was found to exceed its design parameters, with a calculated beam current of 3.9 A from 5.5 A collected by the grids and the projected grid transparency of 70%. The calculated mass utilization efficiency was 93% with a discharge loss of about 160 eV/ion. These performance numbers resulted from the assumption of a $f_a \approx 0.55$ in Brophy's model, which is the fraction of ions impinging on the grids that backflows into the thruster without beam extraction, and a grid transparency of 70%. The maximum current to the grids during these discharge-only mode tests was 7.4 A, which would produce a over 4 A of beam current for grid transparencies as low as 60%. The thruster also produced a remarkably uniform plasma over the 57-cm-diameter grid area, with a measured flatness parameter of 0.84 obtained from a scanning probe mounted inside the discharge chamber immediately upstream of the screen grid. This extremely flat profile permits a wider range of operation of the thruster by providing margin against cross-over and perveance limits across the ion optics diameter.

Subsequent to the discharge-only tests, the high power screen supply was installed and beam extraction experiments performed. The thruster was operated at up to 4 A of beam current at 6500 V, and demonstrated 78% efficiency at 7500 sec ISP and 25 kW of power, and over 81% thruster efficiency measured at 8500 sec ISP. The beam profile was measured by a scanning Faraday probe in the beam external to the thruster, and the a flatness parameter of 0.82 was confirmed. A series of measurements of the effective grid transparency and discharge loss showed that the as-manufactured grids had a transparency of only about 60%, which caused the discharge loss to increase from the projected value to about 185 eV/ion. However, the value of f_a used in Brophy's model was found to be 0.5, in excellent agreement with the value used in the modeling. The NEXIS discharge chamber also demonstrated a mass utilization efficiency of well over 90%, which contributed significantly to the high overall thruster efficiency.

II. Thruster Configuration

The discharge chamber design and the discharge loss analysis for the NEXIS thruster was performed using a JPL model modified from reference [10] to include hollow cathode effects. This model requires some knowledge of the plasma parameters in the discharge, but benchmarking the code against the NSTAR results demonstrated good agreement with the experimental results from the Extended Life Test¹¹ and provided reasonable assumptions for the plasma temperature and profile shape. The LM thruster discharge chamber is 65 cm in diameter at the grid plane and uses 6 ring-cusps to provide magnetic confinement of the plasma. The thruster is designed with a length to diameter ratio slightly larger than NSTAR, but with a much larger diameter and an even number of magnet rings. The LM thruster was tested with flat carbon-carbon (CC) composite grids, whereas the next generation NEXIS thruster³ will use dished CC grids in preparation for handling launch vibrations. The region at the periphery of the carbon-carbon grids near the anode surface is masked to 57 cm in diameter so that the very low plasma density region in the fringing magnetic-cusp field near the wall does not affect the ion optics performance by producing “cross-over ions” or permit unionized propellant from this low plasma density region to leak through the grid. The LM thruster is shown in Fig. 1 during assembly without the carbon grids attached, and during installation in the vacuum chamber with the grids attached. For this series of tests, a conventional B-type “1/2” dispenser cathode with a graphite keeper was used in the discharge chamber and a scanning Faraday probe aligned on-axis for beam profile measurements. The LM thruster cathode design was essentially scaled up from the NSTAR thruster cathode.

The discharge chamber model predicted a discharge loss of about 170 eV/ion for the NEXIS design at a screen grid transparency of 70% and a mass utilization efficiency of 90%. Plasma discharge stability analysis¹² indicated that a four ring-cusp design would be marginal if the discharge loss exceeded 200 eV/ion and discharge current was in excess of about 31 A. Since this would limit the thruster to below 3.8 A of beam current for a nominal 25 V discharge, a six-ring design that provides sufficient anode area to stabilize the discharge at high currents was selected. The analysis indicated that even if the discharge current exceed 35 A in order to produce the desired beam current, the thruster would operate stably. The field produced by the samarium-cobalt magnet rings was designed to minimize primary electron loss at the cusps and ion loss between the cusps, and the even number of cusps reduces the on-axis magnetic field compared to the 3-ring NSTAR design, which greatly improves the plasma profile. The design electrical parameters for the NEXIS thruster are given in Table 1.

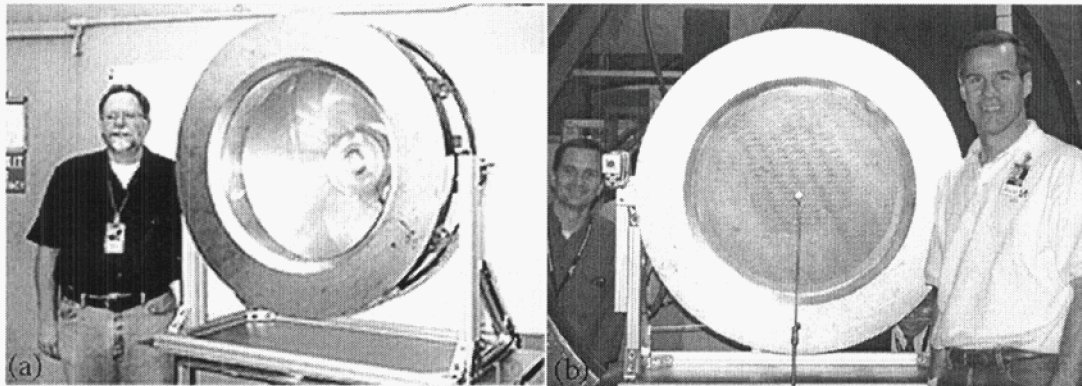


Figure 1. NEXIS LM thruster during assembly (a) and during installation in the vacuum facility (b).

Table 1. Electrical design points for the NEXIS thruster.

Supply	Voltage (V)	Current (A)
Cathode Heater	≤ 15	≤ 10
Cathode Keeper	≤ 30 (650 V, 10 μ sec pulse)	≤ 4
Discharge	24 – 27	15 – 30
Screen Grid	2400 – 7700	2.2 – 4.2
Accel grid	≤ 900	≤ 0.2
Neutralizer Heater	≤ 15	≤ 10
Neutralizer Keeper	≤ 30 (650 V, 10 μ sec pulse)	≤ 4

The internal magnetic field of the discharge chamber was measured using axial and radial Hall probes mounted on a two-axis, computer-controlled positioning system. The r -axis stage of the positioning system was carefully aligned with the downstream cylinder magnet ring and the z -axis was aligned with the thruster centerline using a laser level. Data were collected at 5 mm intervals on a mesh inside the discharge chamber but without the cathode assembly. The cathode assembly contains no magnetic materials, so it is not expected to influence the magnetic field generated by the six magnet rings. The uncertainty in the relative probe positioning is 1 mm and the uncertainty in absolute alignment with the thruster axis and rear discharge chamber wall is ± 1 mm.

Contour plots of the magnetic field magnitude calculated with Maxwell 2D and that measured in the laboratory model thruster are shown in Figure 2 in solid red and dotted blue, respectively. The innermost contour in the discharge chamber is 5 Gauss, and subsequent contours are in 10 G increments starting with 10 Gauss. The 50 Gauss contour line, shown in bold green, is the minimum field strength line that is closed along the entire anode surface. The physical boundaries inside the thruster are shown in black on the plot. The cathode orifice is at a magnetic field strength of about 78 Gauss. The measured and calculated field strengths agree well except along the centerline near the cathode. The fluctuations in the calculated contours appear to be due to discretization of the calculated values, so the discrepancy is probably an artifact of the contour-plotting algorithm.

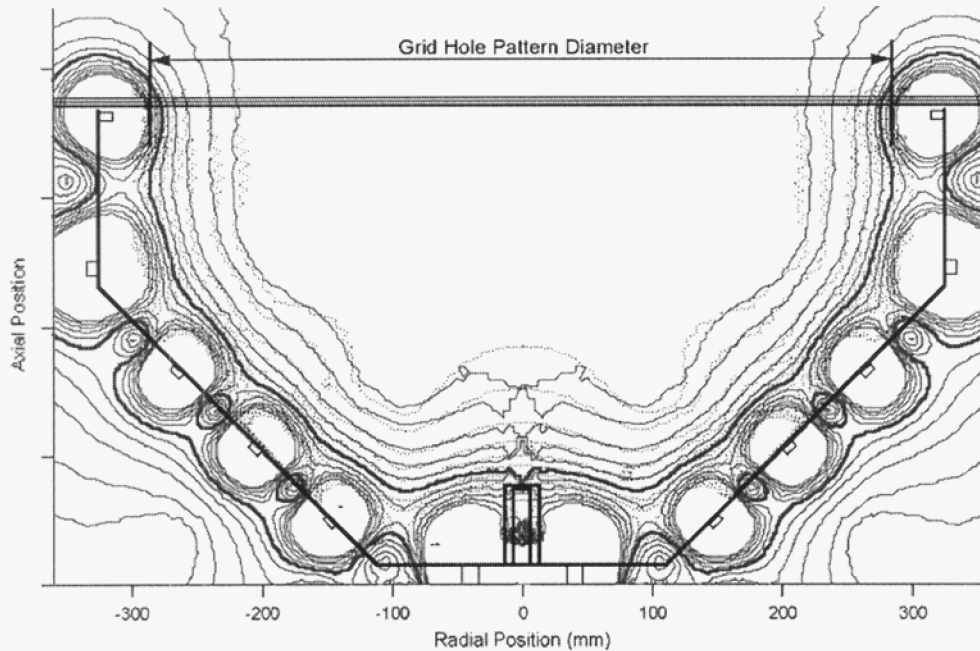


Figure 2. Comparison of measured and calculated magnetic field contours.

III. Thruster Performance

The laboratory model thruster was tested in the JPL “patio chamber” vacuum system. This chamber is 3 m in diameter and 10 m long and is pumped by 6 cryopumps that provide a xenon pump speed of 100,000 L/s. The facility base pressure was $< 1E-7$ Torr, and the pressure with full power flow rates was $1E-5$ Torr. With the main flow lowered to simulate beam extraction the chamber pressure was on the order of $3E-6$ Torr. The xenon propellant was supplied by a feed-back controlled laboratory feed system and measured with flowmeters calibrated to within 0.5%. Laboratory power supplies were wired in the configuration shown in Fig. 1b of reference [1]. Currents and voltages were measured with calibrated shunts and an Optomux-based computer data system.

Discharge chamber operation with beam extraction was simulated first in “discharge-only” tests using the method described in reference [1]. Cathode common was biased 25V positive with respect to facility ground to prevent electrons from escaping the discharge chamber. The grids were biased 20V negative with respect to cathode common to repel electrons, and the ion current to the screen grid and the accelerator grid were measured independently. The actual ion current leaking through the grids due to the small applied-bias was also monitored, but was found to be only about 1.4% of the ion current collected by the two grids. The simulated beam current, i.e. that expected when actually applying the high voltage to the discharge chamber, was calculated from

$$(J_b)_{sim} = (J_s + J_a + J_b)\phi_i \quad (1)$$

Optics simulations of the preliminary NEXIS grid design using the code CEX2D predicted an ion transparency of about 0.7 with beam extraction. The terms on the right-hand-side of Eq. 1 in parentheses represent the total ion current toward the optics, J_g , and it was assumed that 70% of this current would be extracted under normal operating conditions. The grid masking reduces this somewhat because the grid transparency beyond a radius of 28.5 cm is zero, and this turned out to be a finite effect when the discharge-only data was compared to beam-extraction data.

The actual grid transparency to ions without high voltage is given by the expression

$$\phi_i = (f_a J_a + J_s)/(J_s + J_a + J_b) \quad (2)$$

Brophy found¹ that the fraction of ions striking the accel grid that leave the discharge chamber, f_a , was approximately 0.55 for NSTAR-like 30 cm optics on a J-series engine. A value of $f_a=0.5$ was assumed for the NEXIS optics in the analysis below, primarily because the accel grid length to diameter of the CC grids tested is nearly identical to the J-series ion optics and neutral transport is likely similar between the two. The actual value of f_a is shown in the next section based on the beam extraction experiments, but we find that $f_a = 0.45$ to 0.55 bounded the simulated current levels well.

The simulated propellant efficiency (excluding the neutralizer cathode) is given by

$$(\eta_m)_{sim} = \frac{(\phi_i J_g)}{\dot{m} + J_g \left(\frac{1-\phi_i}{\phi_i} \right)} \quad (3)$$

The denominator of this expression represents the effective mass flow rate into the chamber. This consists of the flow injected and the flux of ions returning as neutrals after striking the grids, which would have been extracted as ions with high voltage applied. Simulated beam extraction therefore requires injected mass flow rates substantially lower than those for operation with beam extraction. The discharge loss is calculated in the normal way from the total discharge power divided by the beam current:

$$\eta_d = \frac{(J_D V_D + J_K V_K)}{(J_B)_{sim}} \quad (4)$$

A. Discharge Efficiency Results

Performance curves (discharge loss versus propellant utilization efficiency) were calculated from the discharge-only test data using Eqs. 3 and 4, and are shown in Figure 3. These curves were obtained by varying cathode flow rate, main flow rate and discharge current to maintain a constant simulated beam current of 3.9 A assuming a screen grid transparency of 70% and constant discharge voltages of 24 or 25 V. The two sets of curves at a given discharge voltage show the effect of a different assumed fraction of ions escaping the discharge chamber as neutrals after striking the accelerator grid (2 values of f_a). The performance shown here is excellent; it is less than or equal to the conservative values of 170 eV/ion at a propellant efficiency of 0.91 that were assumed in the initial design and performance calculations.

The cathode flow rate for a propellant efficiency of 0.92-0.93 at a beam current of 3.9 A was 4.45 sccm for 25 V and 5.4 sccm for 24 V. The discharge cathode was operated at flow rates as low

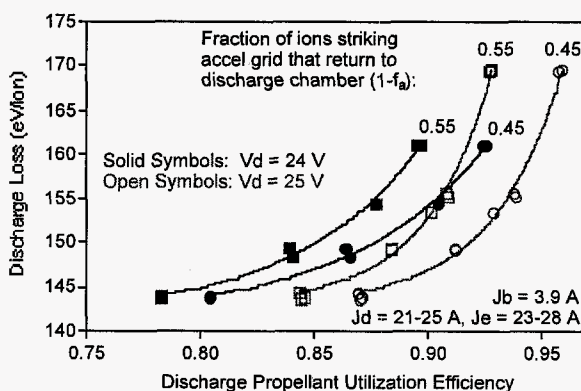


Figure 3. LM thruster discharge loss versus propellant efficiency from the discharge only tests for two discharge voltages and two values of “ f_a ” at 70% grid transparency.

as 3 sccm with no signs of plume mode operation, so a nominal flow of 4-5.5 sccm provides adequate margin. Cathode flow rates higher than about 6 sccm will likely result in discharge voltages that are too low for efficient discharge operation.

As expected, the results show that higher propellant utilization efficiency can be achieved with a modest increase in discharge loss. It is considered reasonable to baseline a propellant efficiency of 0.93 for NEXIS for the nominal operating point because the double ion content at these values was found during beam extraction experiments to be less than 10%. The results also show that there is a relatively small performance difference between a 24 V discharge and a 25 V discharge. As we learn more about what drives cathode keeper erosion from the thruster modeling efforts, we can choose a different discharge voltage or discharge current for a given operating point without a significant penalty in discharge loss.

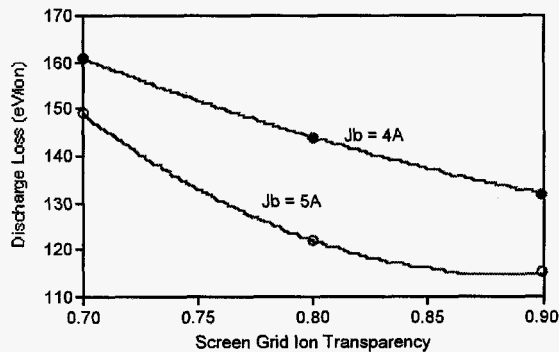


Figure 4. Discharge loss versus screen grid transparency for two beam current levels based on the discharge only results. Improvements in screen grid transparency are essential to reducing the discharge loss in the thruster.

Modifications to the screen grid design to produce a higher transparency, such as thinner grids or shaped holes, can significantly reduce the discharge loss and improves the thruster efficiency. The data collected during these tests were used to estimate the performance gains associated with higher screen transparency at beam currents of 4 and 5 A. Figure 4 shows the calculated discharge loss as a function of grid transparency for these higher beam currents. An improvement in the grid transparency from the assumed 70% to 80% results in a 20% reduction in the discharge loss. Techniques to improve the grid transparency are under consideration to obtain this benefit.

The discharge-only assumptions and results were compared to data obtained from the LM thruster with high voltage beam extraction. Figure 5 shows the measured performance curves from beam extraction tests and the simulated results from the discharge-only

theory. We see that the assumption of the value of f_a of 0.5 provides excellent agreement with the beam data, which validates the use of Brophy's original data for f_a . However, the measured screen transparency was only about 58% at 7500 sec Isp, which is significantly below the assumed value of 0.7. This difference is attributed to a thicker as-manufactured screen grid than that analyzed in the design phase, and the affect of masking the edge of the grid.

Increasing the screen transparency from the observed 58% back to 70% significantly decreases the discharge loss. Figure 6 shows the projected improvement in the performance curves from the model using the measured parameters from these tests. The projected performance results are slightly better than the 170 eV/ion at 91% propellant efficiency that was predicted by the original discharge chamber design model.

B. Plasma Uniformity

A single Langmuir probe was inserted into the discharge chamber of the NEXIS laboratory model thruster close to the screen grid to obtain radial profiles of ion flux and plasma parameters during discharge mode only operation. Ion current profiles were obtained at a fixed negative bias voltage with respect to cathode common. This allowed for determination of the beam flatness parameter, providing an indication of primary electron confinement and plasma uniformity of the lab model discharge chamber design. Current-voltage characteristics were also generated at five different radial locations to allow determination of the plasma density and electron temperature.

The probe consists of a cylindrical 1-mm diameter, 7-mm long, tungsten wire protruding

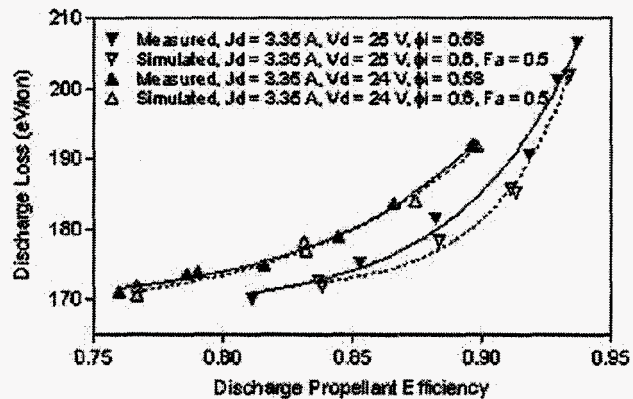


Figure 5. Comparison of the discharge loss versus propellant efficiency from the beam extraction tests and the discharge only tests. The assumed value of f_a of 0.5 provided excellent agreement with the beam data.

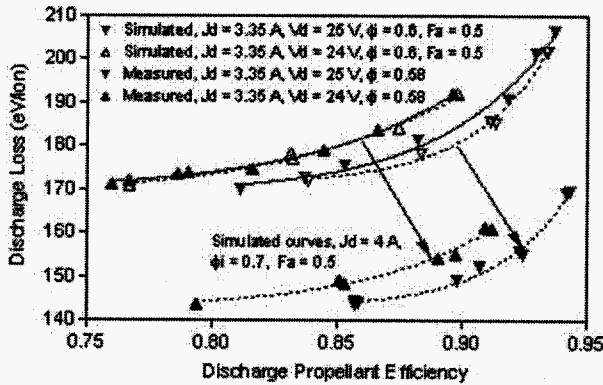


Figure 6. Projected improvement in the discharge loss at higher beam currents if the screen transparency is increased to 70%.

grid, and its position adjusted by means of a computer controlled Velmex Stepper Motor driven stage. The total translation allowed by the stage was 37.47 cm from the anode wall, and the stage was operated with a velocity of 2.54 cm/s for all the tests in this report. The stage has a nonlinear acceleration/deceleration profile, and to account for the associated delay, a limit switch was used to signal the start and end of the stage motion. The triggering of the limit switch was read as a separate +/-10 V signal to the A/D card. The zero (docking) position of the probe was located 3.175 cm outside of the anode in the probe collar mounted to the anode wall. The function generator and bias supply were floated at cathode common potential through an isolation transformer. The differential data acquisition system and stepper motor were referenced to the vacuum chamber ground.

Profiles of the ion current from the radially scanning probe taken during the discharge-only tests are shown in Figure 7. The discharge parameters for two characteristic cases tested are shown in Table 2 with the reduced main-gas flow rate for the simulated beam current calculations. During each scan, the probe was inserted into the engine a speed of 2.54 cm per second, pausing for 0.1 seconds at 37.5 cm from the anode wall, and then returning to the probe start location at the same speed. During each probe translation, the probe was biased 20 V negative of cathode common to repel electrons and to collect ion current.

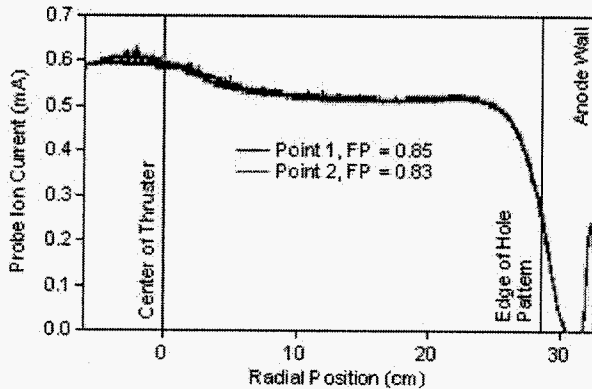


Figure 7. Plasma uniformity measured by the scanning probe for two operating points given in Table 2.

Table 2. Operating parameters and flatness parameter for the beam profile measurements.

Operating Point	J_D [A]	V_D [V]	Main flow [sccm]	Cathode Flow [sccm]	J_B [A]	f_p
1	28.7	26.3	10	5.4	3.95	0.85
2	26.9	27.2	10	4.4	3.85	0.83

from a double bore, 3/16" OD alumina rod. The tungsten wire was spot welded to a stainless steel wire fed through the rod, and connected to a shield junction box at the other end. The probe's output current signal was connected to the data acquisition system through a low-pass filter to remove high frequency noise picked up from the translation stage motor. The signal was measured across a 2-k Ω shunt resistor through a 10:1 voltage divider, and read into a National Instruments A/D card as a differential +/-10 V signal. For the ion saturation only traces, the gain of the A/D card was adjusted to +/-1 V. The probe was biased with respect to cathode common using a KEPCO bipolar power supply with a +/-100V capability. For the ion saturation profiles, the voltage was set to a -20V, with respect to cathode common. The probe was inserted into the engine just upstream of the screen

The ion current profiles in Fig. 7 represent the ion flux to the upstream screen grid, and provide a good indicator of beam (plasma) uniformity and therefore a flatness parameter. The flatness parameter is defined as

$$f_p = J_{i,ave} / J_{i,max} \quad (5)$$

Table 2 lists the flatness parameter for two of the simulated operating points investigated. The thruster demonstrated a remarkable flatness parameter exceeding 0.8. This is indicative of the nearly optimal discharge chamber design, which was achieved without any experimental or empirical iterations using a discharge chamber model developed at JPL. Experiments with beam extraction confirmed these flatness results.

C. Plasma parameters

The probe used in the NEXIS LM thruster initial tests was also used as a classic Langmuir probe to measure the plasma density and electron temperature near the grids. However, the probe produced a non-classical looking current versus voltage traces, as illustrated in Figure 8, where both the ion and electron portions of the I-V trace showed significant slope. This behavior is caused by the expansion of the current collecting sheath area when large probes are used in low-density plasmas. This "thick-sheath" regime can be analyzed using the techniques developed by Laframboise¹³, who addressed the case of a cylindrical probe in a cold, collisionless stationary plasma where the probe bias increases the sheath area sufficiently to affect the collected ion or electron current.

Laframboise showed that the ion current collected by a probe biased below the floating potential in the thick-sheath regime is described by:

$$I = \xi n_i e \sqrt{\frac{kT_e}{2\pi M}} A \quad (6)$$

where ξ is a dimensionless current correction depending on the probe size, plasma density and temperature. Laframboise determined ξ numerically by solving the particle momentum and Poisson's equations to account for varying sheath sizes and particle orbits. Probe analysis in the literature usually addresses the case of small cylindrical probes with a ratio of the radius to the debye length of less than about 3. In this case, Steinbrüchel¹⁴ determined from fits to Laframboise's results that ξ is given to within 3% error by:

$$\xi = \sqrt{\frac{1.27 V}{T_e}} \quad (7)$$

The plasma density can be found¹² from Eqs. 6 and 7 by evaluating the slope of the probe characteristics in the ion collection region by the expression:

$$n_i = \frac{1.96 \times 10^{10}}{A} \sqrt{\left(\frac{dI^2}{dV}\right) M} \quad (8)$$

where I is in mA, n_i is in cm^{-3} , M is in atomic mass unit (AMU), and V is in volts.

However, the relatively large probe used in the NEXIS experiments had a ratio of radius to debye length (r/λ_D) of between 10 and 20, and Eq. 8 does not provide accurate results in this range. Fortunately, Laframboise also analyzed the change in ξ as a function of the probe bias divided by the electron temperature for different values of the probe radius to the Debye length. For $r/\lambda_D \geq 10$, a fit to his graphical results in Figure 40 of reference[13] gives

$$\xi = 0.046 \frac{V}{T_e} + 1.58 \quad (8)$$

Using Eqs. 1 and 8, the probe current is

$$I = 1.83 \times 10^{-2} \frac{n e^{3/2} A}{\sqrt{M}} + 1.58 \quad (9)$$

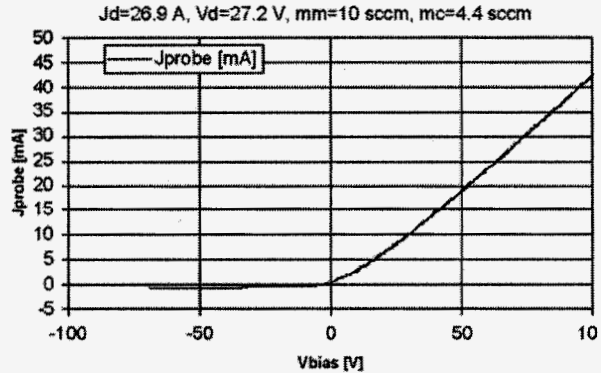


Figure 8. Current versus from the discharge chamber plasma probe showing lack of an electron saturation region.

This expression is in MKS units. Taking the derivative of Eq. 9 with respect to the bias voltage, solving for the plasma density, and converting into more useful units gives:

$$n = 3.5 \times 10^{11} \frac{\sqrt{M}}{A} \frac{dI}{dV} \quad (10)$$

where n_i is the ion density in cm^{-3} , M is the ion mass in AMU, A is the probe area in cm^2 , and dI/dV is in mA per volt.

The plasma density calculated using Eq. 10 is found by first evaluating the slope of the ion current with voltage, which was 0.0055 mA/V as shown in Figure 9. For a probe area of 0.22 cm^2 , Eq. 10 produces a plasma density of $1 \times 10^{11} \text{ cm}^{-3}$. This is very close to the $1.13 \times 10^{11} \text{ cm}^{-3}$ value estimated from the total grid current measurements and the plasma profile made during this scan, and is certainly within the errors expected of this type of analysis¹⁵. In fact, the location of the probe near the screen grid guarantees that it is not really the stationary plasma analyzed by Laframboise. In the thruster near the grids, the pre-sheath effects will modify the effective probe collection area and change the density predicted in addition to the bias-effects discussed here.

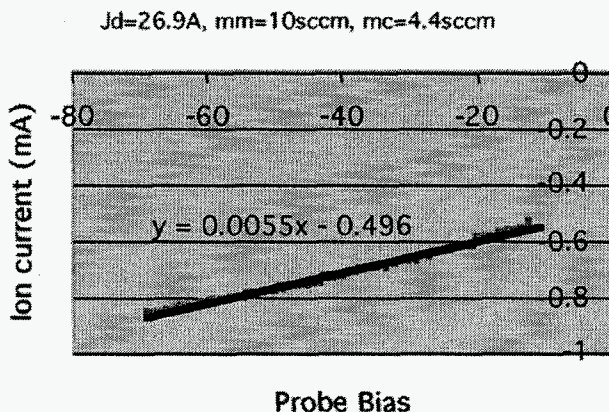


Figure 9. Fit to the linear ion current regime probe data.

Calculations of the electron temperature were also made by attempting to fit an exponential to a portion of the IV curve above the floating potential. For a Maxwellian distribution of electrons, the electron temperature is equivalent to the reciprocal of the slope of the natural log of the fit. Overall, the exponential fits to the current-voltage data were generally poor, and therefore estimates of electron temperature are not particularly accurate.¹⁵ Nevertheless, radial profiles of the electron temperature from this data are shown in Figure 10. At low power and higher main flows, the electron temperature was in the 3 to 4 eV range. At high propellant efficiencies and high power, the electron temperature was observed to be on the order of 5 eV near the screen grid.

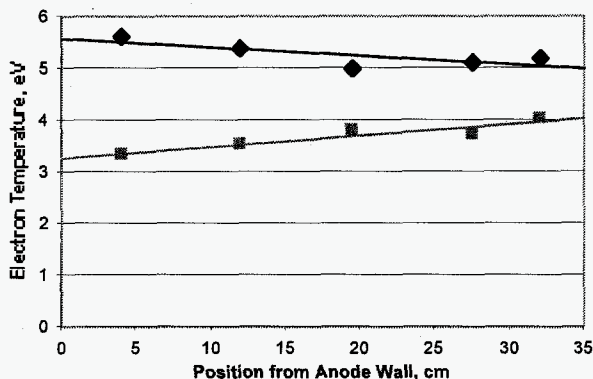


Figure 10. Radial profiles of electron temperature for two test cases representing different discharge conditions.

modeling effort that provided both the chamber design and the performance predictions. The discharge-only mode tests were shown to be extremely successful in predicting the ultimate thruster performance with beam extraction once the model factor f_a was benchmarked. If a better estimate of the grid transparency had been available, the discharge loss predictions from Brophy's model would have been within a few percent. The thruster operated over its design discharge parameters and flow rates without problem, and generated over 3.9 A of beam current at propellant efficiencies over 90% with less than 30 A of discharge current. The plasma profile was found to be extremely flat ($f_p > 0.8$) due to the proper discharge chamber design, which enhances both the performance and life of the ion optics.

IV. Conclusion

The NEXIS discharge chamber design achieved all of the design goals on the first try without the need for experimental iterations. This can be attributed to the discharge plasma

Acknowledgments

The research described in this paper was carried out by the Jet Propulsion Laboratory, California Institute of Technology, under a contract with the National Aeronautics and Space Administration in support of Project Prometheus.

References

- ¹J.R. Brophy, "Simulated Ion Thruster Operation Without Beam Extraction," AIAA 90-2655, 21st International Electric Propulsion Conference, Orlando, FL, 1990.
- ²J. Polk, et al., "An Overview of the Nuclear Electric Xenon Ion System (NEXIS) Program", AIAA-2003-4713, 40th AIAA Joint Propulsion Conference, Fort Lauderdale, FL, July 11-14, 2004.
- ³T. Randolph and J. Polk, "An Overview of the Nuclear Electric Xenon Ion System (NEXIS) Activity", AIAA-2004-3450, 40th AIAA Joint Propulsion Conference, Fort Lauderdale, FL, July 11-14, 2004.
- ⁴J. Brophy, "NASA's Deep Space 1 Ion Engine", Rev. Sci. Instrum. **73** (2002) p.1071-1078
- ⁵John R. Beattie, "XIPS Keeps Satellites on Track", The Industrial Physicist, June 1998.
- ⁶J.S. Sovey, "Improved Ion-Containment Using a Ring-Cusp Ion Thruster", AIAA Paper 82-1928, Nov. 1982.
- ⁷J.R. Beattie and R.L. Poeschel, "Ring-Cusp Ion Thrusters", IEPC Paper 84-71, May 1984.
- ⁸J.N. Matossian and J.R. Beattie, "Characteristics of Ring-Cusp Discharge Chambers", J. Propulsion and Power, **7**, pg. 968-974, Nov. 1991.
- ⁹S. Snyder and J. Brophy, "Performance Characterization and Vibration Testing of 30-cm Carbon-Carbon Ion Optics", AIAA-2004-3959, 40th AIAA Joint Propulsion Conference, Fort Lauderdale, FL, July 11-14, 2004.
- ¹⁰J.R. Brophy, "Ion Thruster Performance Model", NASA CR-174810, Ph.D. Thesis, Colorado State University, Dec. 1984.
- ¹¹A. Sengupta, J. Brophy, and K. Goodfellow, "Status of the Extended Life Test of the Deep Space 1 Flight Spare Ion Engine after 30,352 Hours of Operation, AIAA-2003-4558, 40th AIAA Joint Propulsion Conference, Fort Lauderdale, FL, July 11-14, 2004.
- ¹²D.M. Goebel "Ion Source Discharge Performance and Stability", Physics of Fluids, **25** (1982) 1093.
- ¹³J.G. Laframboise, UTIAS Report #100, University of Toronto, 1966.
- ¹⁴C. Steinbrüchel, J. Electrochem. Soc. **130** (1983) p.648.
- ¹⁵I.D. Sudit and R.C. Woods, "A study of the accuracy of various Langmuir probe theories", J. Appl. Phys., **76** (8), p.4488-4494 (1994).

End of File

